Annals of the University of Craiova, Mathematics and Computer Science Series
Volume 42(1), 2015, Pages 211–225
ISSN: 1223-6934

A domain decomposition method for boundary element approximations of the elasticity equations

Abdellatif Ellabib and Abdeljalil Nachaoui

Abstract. In this paper, we discuss a domain decomposition method to solve linear elasticity problems in complicated 2-D geometries Ω. We describe in details algebraic system corresponding to Dirichlet-Neumann and Schwarz methods. The alternating iterative algorithm obtained is numerically implemented using the boundary element method. The stopping and accuracy criteria, and two type of domain are investigated which confirm that the iterative algorithm produces a convergent and accurate numerical solution with respect to the number of iterations.

2010 Mathematics Subject Classification. Primary 65M12; Secondary 65M55.
Key words and phrases. Dirichlet-Neumann method, overlapping domain decomposition, Boundary element method, Elasticity problems.

1. Introduction

Domain decomposition ideas have been applied to a wide variety of problems. We could not hope to include all these techniques in this work. For an extensive survey of recent advances, we refer to the proceedings of the annual domain decomposition meetings see *http://www.ddm.org*. Domain decomposition algorithms is divided into two classes, those that use overlapping domains, which refer to as Schwarz methods, and those that use non-overlapping domains, which we refer to as substructuring.

Any domain decomposition method is based on the assumption that the given computational domain Ω is decomposed into subdomains Ω_i, $i = 1, \dots, M$, which may or may not overlap. Next, the original problem can be reformulated upon each subdomain Ω_i, yielding a family of subproblems of reduced size that are coupled one to another through the values of the unknowns solution at subdomain interfaces. Fruitful references can be found in [17, 15, 18, 19, 20].

Domain decomposition for contact problems has been applied by many authors (see, for example, surveys [2, 5, 8, 13]. A numerical study of elasticity equations by domain decomposition method combined with finite element method was treated in [10, 11, 6, 9, 12]. A symmetric boundary element analysis with domain decomposition is studied in [7, 16].

The numerical approach based on the overlapping domain decomposition was used for biharmonic equation in two overlapping disks [1] and for Poisson equation [4].

We have chosen to associate the Dirichlet-Neumann and Schwarz methods with the direct boundary element method. Indeed, it only requires the discretization of the boundaries of the subdomains. This technique of coupling reduces the number of unknowns and the time of computing. It has been used successfully for semiconductors simulation [14].

This paper has been presented at Congrès MOCASIM, Marrakech, 19-22 November 2014.

We consider a linear elasticity material which occupies an open bounded domain $\Omega \subset \mathbb{R}^2$, and assume that Ω is bounded by $\Gamma = \partial\Omega$. We also assume that the boundary consists of two parts $\Gamma = \Gamma_1 \cup \Gamma_2$ where Γ_1 and Γ_2 are not empty and $\Gamma_1 \cap \Gamma_2 = \emptyset$ where Ω is not necessarily circular or rectangular.

Let $\mathcal{V} = (u, v)$ the displacement vector and $\mathcal{S} = (t, s)$ the traction vector governed by the following linear elasticity problem

$$\begin{cases} G\Delta u + \dfrac{G}{1-2\nu}\left(\dfrac{\partial^2 u}{\partial x^2} + \dfrac{\partial^2 v}{\partial x \partial y}\right) = 0 \text{ in } \Omega, \\ G\Delta v + \dfrac{G}{1-2\nu}\left(\dfrac{\partial^2 u}{\partial x \partial y} + \dfrac{\partial^2 v}{\partial y^2}\right) = 0 \text{ in } \Omega \\ u = \tilde{u}, \;\; v = \tilde{v} \quad \text{on } \Gamma_1 \\ t = \tilde{t}, \;\; s = \tilde{s} \quad \text{on } \Gamma_2 \end{cases} \tag{1}$$

with G and ν the shear modulus and Poisson ratio, respectively, and where $\tilde{u}$, $\tilde{v}$, $\tilde{t}$ and $\tilde{s}$ are the prescribed quantities.

The main body of this paper begins a description of Dirichlet-Neumann and Schwarz methods for elasticity equations (1), in section 2. Integral formulation and boundary element method are also exposed in subsection 3.1 and 3.2. The technique to obtain algebraic systems on each subdomain for Dirichlet-Neumann and Schwarz methods is detailed in section 4. Two algorithm to implement domain decomposition method combined with boundary element for elasticity equations (1) are presented, and numerical results in the case of 2-D complicated geometries are given in section 5. The paper ends with conclusion in section 6.

2. Domain decomposition techniques

In order to use domain decomposition to linear elasticity, we describe, in this section, Dirichlet-Neumann and Schwarz methods.

2.1. Dirichlet-Neumann substructuring method. We decompose Ω into two non-overlapping subdomains Ω_1 and Ω_2 such that $\Omega = \Omega_1 \cup \Omega_2$, and denote by $\Gamma_{12} = \partial\Omega_1 \cap \partial\Omega_2$ the common interface between Ω_1 and Ω_2. We can write this method as follows.

- Step 1. Specify an initial $\Lambda^0 = (\lambda^0, \beta^0)$ on interface Γ_{12} and $k = 0$.
- Step 2. Solve the mixed well-posed direct problem

$$\begin{cases} G\Delta u_1^k + \dfrac{G}{1-2\nu}\left(\dfrac{\partial^2 u_1^k}{\partial x^2} + \dfrac{\partial^2 v_1^k}{\partial x \partial y}\right) = 0 \text{ in } \Omega_1 \\ G\Delta v_1^k + \dfrac{G}{1-2\nu}\left(\dfrac{\partial^2 u_1^k}{\partial x \partial y} + \dfrac{\partial^2 v_1^k}{\partial y^2}\right) = 0 \text{ in } \Omega_1 \\ u_1^k = \tilde{u}, \;\; v_1^k = \tilde{v} \text{ on } \Gamma_1 \cap \partial\Omega_1 \\ t_1^k = \tilde{t}, \;\; s_1^k = \tilde{s} \text{ on } \Gamma_2 \cap \partial\Omega_1 \\ u_1^k = \lambda^k, \;\; v_1^k = \beta^k \text{ on } \Gamma_{12} \end{cases} \tag{2}$$

to determine the traction $\mathcal{S}_1^k = (t_1^k, s_1^k)$ on the interface Γ_{12}.

- Step 3. Solve the mixed well-posed direct problem

$$\begin{cases} G\Delta u_2^k + \dfrac{G}{1-2\nu}\left(\dfrac{\partial^2 u_2^k}{\partial x^2} + \dfrac{\partial^2 v_2^k}{\partial x \partial y}\right) = 0 \text{ in } \Omega_2 \\ G\Delta v_2^k + \dfrac{G}{1-2\nu}\left(\dfrac{\partial^2 u_2^k}{\partial x \partial y} + \dfrac{\partial^2 v_2^k}{\partial y^2}\right) = 0 \text{ in } \Omega_2 \\ u_2^k = \tilde{u}, \;\; v_2^k = \tilde{v} \text{ on } \Gamma_1 \cap \partial\Omega_2 \\ t_2^k = \tilde{t}, \;\; s_2^k = \tilde{s} \text{ on } \Gamma_2 \cap \partial\Omega_2 \\ t_2^k = -t_1^k, \;\; s_2^k = -s_1^k \quad \text{ on } \Gamma_{12} \end{cases} \tag{3}$$

  to determine the displacement $\mathcal{V}_2^k = (u_2^k, v_2^k)$ on the interface Γ_{12}.
- Step 4. Update $\Lambda^{k+1} = (\lambda^{k+1}, \beta^{k+1})$ on the interface Γ_{12} by

$$\begin{cases} \lambda^{k+1} = \theta u_2^k + (1-\theta)\lambda^k \text{ on } \Gamma_{12} \\ \beta^{k+1} = \theta v_2^k + (1-\theta)\beta^k \text{ on } \Gamma_{12} \end{cases} \tag{4}$$

- Step 5. Repeat step 2 from $k \geq 0$ until a prescribed stopping criterion is satisfied.

where θ is positive parameter. This algorithm establish the solution of elasticity equations of Problem 1 in Ω as a limit of sequence $(u_1^k, v_1^k, u_2^k, v_2^k)$.

For this algorithm the following stopping criterion is used

$$\max\left(\|\lambda^{k+1} - \lambda^k\|_{L^2(\Gamma_{12})}, \|\beta^{k+1} - \beta^k\|_{L^2(\Gamma_{12})}\right) < Tol, \tag{5}$$

where Tol is a prescribed tolerance.

2.2. Schwarz overlapping method. We decompose Ω into two overlapping subdomains Ω_1 and Ω_2 such that $\Omega = \Omega_1 \cup \Omega_2$, and denote by $\Gamma_{11} = \partial\Omega_1 \cap \overline{\Omega_2}$ and $\Gamma_{22} = \partial\Omega_2 \cap \overline{\Omega_1}$. This method is summarized in the following.

- Step 1. Specify an initial $\mathcal{V}_2^0 = (u_2^0, v_2^0)$ on Γ_{11} and $k = 0$.
- Step 2. Solve the mixed well-posed direct problem

$$\begin{cases} G\Delta u_1^{k+1} + \dfrac{G}{1-2\nu}\left(\dfrac{\partial^2 u_1^{k+1}}{\partial x^2} + \dfrac{\partial^2 v_1^{k+1}}{\partial x \partial y}\right) = 0 \text{ in } \Omega_1 \\ G\Delta v_1^{k+1} + \dfrac{G}{1-2\nu}\left(\dfrac{\partial^2 u_1^{k+1}}{\partial x \partial y} + \dfrac{\partial^2 v_1^{k+1}}{\partial y^2}\right) = 0 \text{ in } \Omega_1 \\ u_1^{k+1} = \tilde{u}, \;\; v_1^{k+1} = \tilde{v} \text{ on } \Gamma_1 \cap \partial\Omega_1 \\ t_1^{k+1} = \tilde{t}, \;\; s_1^{k+1} = \tilde{s} \text{ on } \Gamma_2 \cap \partial\Omega_1 \\ u_1^{k+1} = u_2^k, \;\; v_1^{k+1} = v_2^k \text{ on } \Gamma_{11} \end{cases} \tag{6}$$

  to determine the displacement $\mathcal{V}_1^{k+1} = (u_1^{k+1}, v_1^{k+1})$ and traction $\mathcal{S}_1^{k+1} = (t_1^{k+1}, s_1^{k+1})$ on the boundary of Ω_1.
- Step 3. Compute the displacement $\mathcal{V}_1^{k+1} = (u_1^{k+1}, v_1^{k+1})$ on Γ_{22} as an internal displacement of linear elasticity equations in Ω_1.
- Step 4. Solve the mixed well-posed direct problem then

$$\begin{cases} G\Delta u_2^{k+1} + \dfrac{G}{1-2\nu}\left(\dfrac{\partial^2 u_2^{k+1}}{\partial x^2} + \dfrac{\partial^2 v_2^{k+1}}{\partial x \partial y}\right) = 0 \text{ in } \Omega_2 \\ G\Delta v_2^{k+1} + \dfrac{G}{1-2\nu}\left(\dfrac{\partial^2 u_2^{k+1}}{\partial x \partial y} + \dfrac{\partial^2 v_2^{k+1}}{\partial y^2}\right) = 0 \text{ in } \Omega_2 \\ u_2^{k+1} = \tilde{u}, \;\; v_2^{k+1} = \tilde{v} \text{ on } \Gamma_1 \cap \partial\Omega_2 \\ t_2^{k+1} = \tilde{t}, \;\; s_2^{k+1} = \tilde{s} \text{ on } \Gamma_2 \cap \partial\Omega_2 \\ u_2^{k+1} = u_1^{k+1}, \;\; v_2^{k+1} = v_1^{k+1} \text{ on } \Gamma_{22} \end{cases} \tag{7}$$

to determine the displacement $\mathcal{V}_2^{k+1} = (u_2^{k+1}, v_2^{k+1})$ and traction $\mathcal{S}_2^{k+1} = (t_2^{k+1}, s_2^{k+1})$ on the boundary of Ω_2.

- Step 5. Compute the displacement $\mathcal{V}_2^{k+1} = (u_2^{k+1}, v_2^{k+1})$ on Γ_{11} as an internal displacement of linear elasticity equations in Ω_2.
- Step 6. Repeat step 2 from $k \geq 0$ until a prescribed stopping criterion is satisfied.

For this algorithm the following stopping criterion is used

$$\max\left(\|u_1^{k+1} - u_1^k\|_{L^2(\Gamma_{11})}, \|v_1^{k+1} - v_1^k\|_{L^2(\Gamma_{11})}, \|u_2^{k+1} - u_2^k\|_{L^2(\Gamma_{22})}, \|v_2^{k+1} - v_2^k\|_{L^2(\Gamma_{22})}\right) < Tol, \tag{8}$$

where Tol is a prescribed tolerance.

The boundary element method utilizes information on the boundaries of interest, and thus reduces the dimension of the problem by one. The displacements in the domain is uniquely defined by the displacements and tractions on the boundary. In the boundary element method, only the boundary is discretized; hence, the mesh generation is considerably simpler for this method than for space discretization techniques, such as the finite difference method or finite element method. Moreover, the Boundary element method determines simultaneously the boundary displacements and tractions, this allows us to solve problem (2), (3) without the need of further finite difference, as one would employ if using the finite element method or the finite difference method.

For these reasons we have decided in this study to use the boundary element method in order to implement the Dirichlet-Neumann and Schwarz methods.

3. Integral equation formulation and boundary element for elasticity equations

The linear elasticity problem (1) in two-dimensional case can be formulated in integral form [3] as follows

$$\int_\Gamma U_{ij}(P,Q)\{\mathcal{S}\}_j(Q)\,d\Gamma(Q) - \int_\Gamma T_{ij}(P,Q)\{\mathcal{V}\}_j(Q)\,d\Gamma(Q) = \begin{cases} \{\mathcal{V}\}_i(P) \text{ if } P \in \Omega \\ \frac{1}{2}\{\mathcal{V}\}_i(P) \text{ if } P \in \Gamma \end{cases} \tag{9}$$

for $i, j = 1, 2$, where U_{ij} and T_{ij} denote the fundamental displacements and tractions for the two-dimensional isotropic linear elasticity [3]. The boundary integral equations are solved using boundary element method with constant boundary elements. The boundary is divided into N constant elements. Denoting by $\{\mathcal{V}\}^i = \{u^i, v^i\}^T$ and $\{\mathcal{S}\}^i = \{t^i, s^i\}^T$ the displacements and tractions at the i^{th} node. Then, the discretized form of Eq. (9) can be written as $\frac{1}{2}\{\mathcal{V}\}^i + \sum_{j=1}^N \hat{H}^{ij}\{\mathcal{V}\}^j = \sum_{j=1}^N G^{ij}\{\mathcal{S}\}^j$ where G^{ij} and $\hat{H}^{ij}$ are 2×2 matrices such that for $l, m = 1, 2$

$$(G^{ij})_{lm} = \int_{\Gamma_j} U_{lm}(P^i, Q)\,d\Gamma(Q) \text{ and } (\hat{H}^{ij})_{lm} = \int_{\Gamma_j} T_{lm}(P^i, Q)\,d\Gamma(Q)$$

Applying this equation to all the boundary nodal points yields $2N$ equations, which can be set in matrix form as

$$H\,\mathcal{V} = G\,\mathcal{S} \tag{10}$$

where $H = \hat{H} + \frac{1}{2}I$ and I is $2N \times 2N$ identity matrix. The displacements in the interior of Ω can be evaluated using Eq. (9) which after discretization becomes

$$\{\mathcal{V}\}^i = \sum_{j=1}^{N} G^{ij}\{\mathcal{S}\}^j - \sum_{j=1}^{N} \hat{H}^{ij}\{\mathcal{V}\}^j. \tag{11}$$

4. Algebraic systems of Dirichlet Neumann and Schwarz methods

We consider in this work the mixed boundary condition given by Problem (2), (3), (6) and (7). In this case the rearrangement of the unknowns in Eq. (10) is necessary. In order to obtain an algebraic system, we denote the matrices H_i and G_i computed in each subdomain Ω_i by the use of Dirichlet Neumann or Schwarz method. Note that H_i and G_i are geometry dependent matrices and depend on the type of the boundary conditions, but not on their values. Therefore the matrices H_i and G_i do not change during the iterate procedure of domain decomposition method. We suppose that the boundary $\Gamma_j \cap \partial\Omega_i$ is divided into N_j constant elements for $i, j = 1, 2$.

4.1. Alternating algebraic system of Dirichlet-Neumann method. Let the boundary Γ_{12} divided into N_{12} constant elements. Due to the boundary condition of system (2) and (3), the matrices H_i and G_i are decomposed as follows

$$H_i = (H_{\Gamma_1\cap\partial\Omega_i}\ H_{\Gamma_2\cap\partial\Omega_i}\ H_{\Gamma_{12}}) \text{ and } G_i = (G_{\Gamma_1\cap\partial\Omega_i}\ G_{\Gamma_2\cap\partial\Omega_i}\ G_{\Gamma_{12}}) \tag{12}$$

The algebraic systems corresponding to subproblems (2) and (3) take the form

$$\left\{\begin{array}{l} (H_{\Gamma_1\cap\partial\Omega_1}\ H_{\Gamma_2\cap\partial\Omega_1}\ H_{\Gamma_{12}}) \begin{pmatrix} \mathcal{V}_1^k|_{\Gamma_1\cap\partial\Omega_1} \\ \mathcal{V}^k_{1\,|_{\Gamma_2\cap\partial\Omega_1}} \\ \mathcal{V}^k_{1\,|_{\Gamma_{12}}} \end{pmatrix} \\ = (G_{\Gamma_1\cap\partial\Omega_1}\ G_{\Gamma_2\cap\partial\Omega_1}\ G_{\Gamma_{12}}) \begin{pmatrix} \mathcal{S}^k_{1\,|_{\Gamma_1\cap\partial\Omega_1}} \\ \mathcal{S}^k_{1\,|_{\Gamma_2\cap\partial\Omega_1}} \\ \mathcal{S}^k_{1\,|_{\Gamma_{12}}} \end{pmatrix} \\ \\ \mathcal{V}^k_{1\,|_{\Gamma_1\cap\partial\Omega_1}} = \tilde{V}_1,\ \mathcal{S}^k_{1\,|_{\Gamma_2\cap\partial\Omega_1}} = \tilde{S}_1,\ \mathcal{V}^k_{1\,|_{\Gamma_{12}}} = \Lambda^k \end{array}\right. \tag{13}$$

and

$$\left\{\begin{array}{l} (H_{\Gamma_1\cap\partial\Omega_2}\ H_{\Gamma_2\cap\partial\Omega_2}\ H_{\Gamma_{12}}) \begin{pmatrix} \mathcal{V}^k_{2\,|_{\Gamma_1\cap\partial\Omega_2}} \\ \mathcal{V}^k_{2\,|_{\Gamma_2\cap\partial\Omega_2}} \\ \mathcal{V}^k_{2\,|_{\Gamma_{12}}} \end{pmatrix} \\ = (G_{\Gamma_1\cap\partial\Omega_2}\ G_{\Gamma_2\cap\partial\Omega_2}\ G_{\Gamma_{12}}) \begin{pmatrix} \mathcal{S}^k_{2\,|_{\Gamma_1\cap\partial\Omega_2}} \\ \mathcal{S}^k_{2\,|_{\Gamma_2\cap\partial\Omega_2}} \\ \mathcal{S}^k_{2\,|_{\Gamma_{12}}} \end{pmatrix} \\ \\ \mathcal{V}^k_{2\,|_{\Gamma_1\cap\partial\Omega_2}} = \tilde{V}_2,\ \mathcal{S}^k_{2\,|_{\Gamma_2\cap\partial\Omega_2}} = \tilde{S}_2,\ \mathcal{S}^k_{2\,|_{\Gamma_{12}}} = -\mathcal{S}^k{}_{1|_{\Gamma_{12}}}. \end{array}\right. \tag{14}$$

The actualization of Λ^k is given by

$$\Lambda^{k+1} = \theta\mathcal{V}^k{}_{2|_{\Gamma_{12}}} + (1-\theta)\Lambda^k. \tag{15}$$

Let X_1^k and X_2^k be the vectors containing the unknowns values of displacements or tractions on the boundary of subdomains Ω_1 and Ω_2 respectively. They are given by

$$X_1^k = \begin{pmatrix} \mathcal{S}_1^k{}_{|\Gamma_1\cap\partial\Omega_1} \\ \mathcal{V}_1^k{}_{|\Gamma_2\cap\partial\Omega_1} \\ \mathcal{S}_1^k{}_{|\Gamma_{12}} \end{pmatrix} \text{ and } X_2^k = \begin{pmatrix} \mathcal{S}_2^k{}_{|\Gamma_1\cap\partial\Omega_2} \\ \mathcal{V}_2^k{}_{|\Gamma_2\cap\partial\Omega_2} \\ \mathcal{V}_2^k{}_{|\Gamma_{12}} \end{pmatrix}. \tag{16}$$

The matrices A_1 and A_2 are defined by the following

$$A_1 = (-G_{\Gamma_1\cap\partial\Omega_1}\ H_{\Gamma_2\cap\partial\Omega_1}\ \ -G_{\Gamma_{12}}) \text{ and } A_2 = (-G_{\Gamma_1\cap\partial\Omega_2}\ H_{\Gamma_2\cap\partial\Omega_2}\ H_{\Gamma_{12}}). \tag{17}$$

Then the algebraic system of Dirichlet-Neumann associated to problem (2) and (3) is written in the following

$$\begin{aligned} A_1X_1^k &= -H_{\Gamma_1\cap\partial\Omega_1}\tilde{V}_1 + G_{\Gamma_2\cap\partial\Omega_1}\tilde{S}_1 - H_{\Gamma_{12}}\Lambda^k, \\ A_2X_2^k &= -H_{\Gamma_1\cap\partial\Omega_2}\tilde{V}_2 + G_{\Gamma_2\cap\partial\Omega_2}\tilde{S}_2 - G_{\Gamma_{12}}X_1^k{}_{|\Gamma_{12}} \end{aligned} \tag{18}$$

and

$$\Lambda^{k+1} = \theta X_2^k{}_{|\Gamma_{12}} + (1-\theta)\Lambda^k. \tag{19}$$

For simplification, let

$$B_1^k = -H_{\Gamma_1\cap\partial\Omega_1}\tilde{V}_1 + G_{\Gamma_2\cap\partial\Omega_1}\tilde{S}_1 - H_{\Gamma_{12}}\Lambda^k \tag{20}$$

$$B_2^k = -H_{\Gamma_1\cap\partial\Omega_2}\tilde{V}_2 + G_{\Gamma_2\cap\partial\Omega_2}\tilde{S}_2 - G_{\Gamma_{12}}X^k{}_{1|_{\Gamma_{12}}}. \tag{21}$$

The matrices A_1 and A_2 can be factorized in the following

$$A_1 = \mathcal{L}_1\mathcal{R}_1 \text{ and } A_2 = \mathcal{L}_2\mathcal{R}_2$$

where $\mathcal{L}_1$, $\mathcal{L}_2$ are lower triangular matrices and $\mathcal{R}_1$, $\mathcal{R}_2$ are upper triangular matrices. Now from (18) X_1^k and X_2^k can be obtained by backward followed by forward substitutions. This gives arise to the following algorithm :

Algorithm 4.1

(1) Set $k = 0$, choose the initial $\Lambda^0 = (\lambda^0, \beta^0) \in \mathbb{R}^{2N_{12}}$ and a tolerance for the iterative solver
(2) Compute H_i and G_i for subdomains Ω_i for $i = 1, 2$
(3) Compute A_i using Eq. (17) for $i = 1, 2$
(4) Compute $\mathcal{L}_i$ and $\mathcal{R}_i$ (decomposition of A_i) for $i = 1, 2$
(5) Repeat
- Compute the vector containing known boundary values B_1^k using Eq. (20)
- Solve system $\mathcal{L}_1\mathcal{R}_1X_1^k = B_1^k$
- Compute the vector containing known boundary values B_2^k using Eq. (21)
- Solve $\mathcal{L}_2\mathcal{R}_2X_2^k = B_2^k$
- Update $\Lambda^k = (\lambda^k, \beta^k)$ by formula (19)
- $k = k + 1$

Until convergence.

(6) End.

4.2. Alternating algebraic system of Schwarz method. Let the boundary Γ_{ii} divided into N_{ii} constant elements for $i = 1, 2$. The matrices H_i and G_i associated to the system (6) and (7), can be decomposed as follows

$$H_i = (H_{\Gamma_1 \cap \partial\Omega_i} \; H_{\Gamma_2 \cap \partial\Omega_i} \; H_{\Gamma_{ii}}) \text{ and } G_i = (G_{\Gamma_1 \cap \partial\Omega_i} \; G_{\Gamma_2 \cap \partial\Omega_i} \; G_{\Gamma_{ii}}) \tag{22}$$

In order to compute the internal displacements in Ω_i by Eq. (11), we introduce the matrix $\mathcal{I}_i$ which take the form

$$\mathcal{I}_i = (-H_{\Omega_i} \quad G_{\Omega_i}). \tag{23}$$

The algebraic systems obtained from boundary element discretisation of subproblems (6) and (7) take the form

$$\left\{ \begin{array}{l} (H_{\Gamma_1 \cap \partial\Omega_1} \; H_{\Gamma_2 \cap \partial\Omega_1} \; H_{\Gamma_{11}}) \begin{pmatrix} \mathcal{V}_1^{k+1}{}_{|\Gamma_1 \cap \partial\Omega_1} \\ \mathcal{V}_1^{k+1}{}_{|\Gamma_2 \cap \partial\Omega_1} \\ \mathcal{V}_1^{k+1}{}_{|\Gamma_{11}} \end{pmatrix} \\ = (G_{\Gamma_1 \cap \partial\Omega_1} \; G_{\Gamma_2 \cap \partial\Omega_1} \; G_{\Gamma_{11}}) \begin{pmatrix} \mathcal{S}_1^{k+1}{}_{|\Gamma_1 \cap \partial\Omega_1} \\ \mathcal{S}_1^{k+1}{}_{|\Gamma_2 \cap \partial\Omega_1} \\ \mathcal{S}_1^{k+1}{}_{|\Gamma_{11}} \end{pmatrix} \\ \mathcal{V}_1^{k+1}{}_{|\Gamma_1 \cap \partial\Omega_1} = \tilde{V}_1, \; \mathcal{S}_1^{k+1}{}_{|\Gamma_2 \cap \partial\Omega_1} = \tilde{S}_1, \; \mathcal{V}_1^{k+1}{}_{|\Gamma_{11}} = \mathcal{V}_{2\,|\Gamma_{11}}^{k}, \end{array} \right. \tag{24}$$

$$\mathcal{V}_1^{k+1}{}_{|\Gamma_{22}} = \mathcal{I}_1 \begin{pmatrix} \mathcal{V}_1^{k+1}{}_{|\partial\Omega_1} \\ \mathcal{S}_1^{k+1}{}_{|\partial\Omega_1} \end{pmatrix} \tag{25}$$

and

$$\left\{ \begin{array}{l} (H_{\Gamma_1 \cap \partial\Omega_2} \; H_{\Gamma_2 \cap \partial\Omega_2} \; H_{\Gamma_{22}}) \begin{pmatrix} \mathcal{V}_2^{k+1}{}_{|\Gamma_1 \cap \partial\Omega_2} \\ \mathcal{V}_2^{k+1}{}_{2|\Gamma_2 \cap \partial\Omega_2} \\ \mathcal{V}_2^{k+1}{}_{2|\Gamma_{22}} \end{pmatrix} \\ = (G_{\Gamma_1 \cap \partial\Omega_2} \; G_{\Gamma_2 \cap \partial\Omega_2} \; G_{\Gamma_{22}}) \begin{pmatrix} \mathcal{S}_2^{k+1}{}_{|\Gamma_1 \cap \partial\Omega_2} \\ \mathcal{S}_2^{k+1}{}_{|\Gamma_2 \cap \partial\Omega_2} \\ \mathcal{S}_2^{k+1}{}_{|\Gamma_{22}} \end{pmatrix} \\ \mathcal{V}_2^{k+1}{}_{|\Gamma_1 \cap \partial\Omega_2} = \tilde{V}_2, \; \mathcal{S}_2^{k+1}{}_{|\Gamma_2 \cap \partial\Omega_2} = \tilde{S}_2, \; \mathcal{S}_2^{k+1}{}_{|\Gamma_{22}} = \mathcal{V}_1^{k+1}{}_{|\Gamma_{22}}, \end{array} \right. \tag{26}$$

$$\mathcal{V}_2^{k+1}{}_{|\Gamma_{11}} = \mathcal{I}_2 \begin{pmatrix} \mathcal{V}_2^{k+1}{}_{|\partial\Omega_2} \\ \mathcal{S}_2^{k+1}{}_{|\partial\Omega_2} \end{pmatrix}. \tag{27}$$

Let X_i^{k+1}, the vectors containing the unknowns values of displacements or tractions on the boundary of subdomains Ω_i for $i = 1, 2$, have the following form

$$X_i^{k+1} = \begin{pmatrix} \mathcal{S}_i^{k+1}{}_{|\Gamma_1 \cap \partial\Omega_i} \\ \mathcal{V}_i^{k+1}{}_{|\Gamma_2 \cap \partial\Omega_i} \\ \mathcal{S}_i^{k+1}{}_{|\Gamma_{ii}} \end{pmatrix} \tag{28}$$

The matrices A_1 and A_2 are defined for $i = 1, 2$ by the following

$$A_i = (-G_{\Gamma_1 \cap \partial\Omega_i} \; H_{\Gamma_2 \cap \partial\Omega_i} \; - G_{\Gamma_{ii}}) \tag{29}$$

Then the algebraic system of Schwarz method associated to problem (6) and (7) is written in the following

$$A_1 X_1^{k+1} = B_1^k, \; A_2 X_2^{k+1} = B_2^{k+1} \tag{30}$$

where

$$B_1^k = -H_{\Gamma_1\cap\partial\Omega_1}\tilde{V}_1 + G_{\Gamma_2\cap\partial\Omega_1}\tilde{S}_1 - H_{\Gamma_{11}}\mathcal{V}^k_{2\,|\Gamma_{11}} \tag{31}$$

$$B_2^{k+1} = -H_{\Gamma_1\cap\partial\Omega_2}\tilde{V}_2 + G_{\Gamma_2\cap\partial\Omega_2}\tilde{S}_2 - H_{\Gamma_{22}}\mathcal{V}^{k+1}_{1\,|\Gamma_{11}}. \tag{32}$$

The matrices A_1 and A_2 can be factorized in the following $A_1 = \mathcal{L}_1\mathcal{R}_1$ and $A_2 = \mathcal{L}_2\mathcal{R}_2$ where $\mathcal{L}_1$, $\mathcal{L}_2$ are lower triangular matrices and $\mathcal{R}_1$, $\mathcal{R}_2$ are upper triangular matrices. Now from (30) X_1^{k+1} and X_2^{k+1} can be obtained by backward followed by forward substitutions. This gives arise to the following algorithm :

Algorithm 4.2

(1) Set $k = 0$, choose the initial $\mathcal{V}_2^0 \in \mathbb{R}^{2N_{11}}$ given and a tolerance for the iterative solver
(2) Compute H_i and G_i for subdomains Ω_i for $i = 1, 2$
(3) Compute A_i using Eq. (29) for $i = 1, 2$
(4) Compute $\mathcal{I}_i$ using Eq. (23) for $i = 1, 2$
(5) Compute $\mathcal{L}_i$ and $\mathcal{R}_i$ (decomposition of A_i) for $i = 1, 2$
(6) Repeat
  - Compute the vector containing known boundary values B_1^k using Eq. (31)
  - Solve system $\mathcal{L}_1\mathcal{R}_1X_1^{k+1} = B_1^k$
  - Compute internal displacement in subdomain Ω_1 using Eq. (25)
  - Compute the vector containing known boundary values B_2^{k+1} using Eq. (32)
  - Solve $\mathcal{L}_2\mathcal{R}_2X_2^{k+1} = B_2^{k+1}$
  - Compute internal displacement in subdomain Ω_2 using Eq. (27)
  - $k = k + 1$

  Until convergence.
(7) End.

5. Numerical results and discussions

In this section, we illustrate the numerical results obtained using the Dirichlet-Neumann and Schwarz domain decomposition method combined with boundary element method for linear elasticity problem. The comparison of this two domain decomposition method is done in L-shaped domain.

The behavior of the method is investigated evaluating the difference between two consecutive approximations for the displacements solutions and its tractions on the boundary γ given by

$$\begin{array}{l} E_k^i(u) = \|u_i^{k+1} - u_i^k\|_{L^2(\gamma)},\ E_k^i(v) = \|v_i^{k+1} - v_i^k\|_{L^2(\gamma)}, \\ E_k^i(t) = \|t_i^{k+1} - t_i^k\|_{L^2(\gamma)},\ E_k^i(s) = \|s_i^{k+1} - s_i^k\|_{L^2(\gamma)}. \end{array} \tag{33}$$

Based on absolute errors the following stopping criterion is considered for Algorithm 4.2

$$\max(E_k^i(u), E_k^i(v)) < \eta. \tag{34}$$

The stopping criterion for Algorithm 4.1 is

$$\max(E_k(\lambda), E_k(\beta)) < \eta \tag{35}$$

where

$$E_k(\lambda) = \|\lambda^{k+1} - \lambda^k\|_{L^2(\gamma)},\ E_k(\beta) = \|\beta^{k+1} - \beta^k\|_{L^2(\gamma)} \tag{36}$$

where η is a small prescribed positive quantity.

In order to investigate the convergence of the two algorithm, at every iteration we evaluate the accuracy errors defined by

$$\begin{array}{l} G_u^i(k) = \|u_i - u_i^{an}\|_{L^2(\gamma)},\ G_v^i(k) = \|v_i - v_i^{an}\|_{L^2(\gamma)}, \\ G_t^i(k) = \|t_i - t_i^{an}\|_{L^2(\gamma)},\ G_s^i(k) = \|s_i - s_i^{an}\|_{L^2(\gamma)}. \end{array} \tag{37}$$

Note that (34) or (35) express that the sequence (u^k, v^k) converge in sobolev spaces $H^{\frac{1}{2}}(\gamma) \times H^{\frac{1}{2}}(\gamma)$. For all numerical experiments, we take $\eta = 10^{-7}$. Note that we have $\gamma = \Gamma_{12}$ for Algorithm 4.1 and for Algorithm 4.2 $\gamma_i = \Gamma_{ii}$, $i = 1, 2$.

5.1. Example 1. In order to illustrate the performance of the numerical method described above, we solve the linear elasticity problem (1), in two-dimensional L-shaped domain $\Omega = (0,1) \times (0,0.5) \cup (0,0.5) \times (0,1)$. We assume that the boundary is split into two parts $\Gamma_1 = [0,1] \times \{0\} \cup [\frac{1}{2}, 1] \times \left\{\frac{1}{2}\right\} \cup [0, \frac{1}{2}] \times \{1\}$ and $\Gamma_2 = \{1\} \times [0, \frac{1}{2}] \cup \left\{\frac{1}{2}\right\} \times [\frac{1}{2}, 1] \cup \{0\} \times [0,1]$. The exact solution of the direct problem is given by

$$u(x,y) = \frac{1-\nu}{2G}\sigma_0 x,\ v(x,y) = -\frac{\nu}{2G}\sigma_0 y,\ t(x,y) = \sigma_0 n_1,\ s(x,y) = 0 \tag{38}$$

with $\sigma_0 = 1.5 \times 10^{10}$, $G = 3.35 \times 10^{10}$ and $\nu = 0.25$.

This example consists in spliting the domain Ω into two rectangular subdomains $\Omega_1 = (0.5, 1) \times (0, 0.5)$ and $\Omega_2 = (0, 0.5) \times (0, 1)$ with interface $\gamma = \{0.5\} \times [0, 0.5]$.

The evolution of behavior errors as a function of the iteration number using Algorithm 4.1 is plotted in Fig. 1.

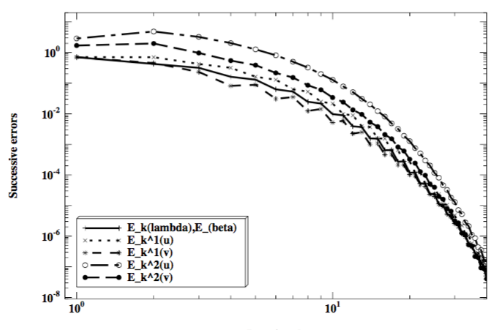

FIGURE 1. The behavior errors given by (33), (35) as a function of the number of iterations k on interface γ for Example 1.

Fig. 2(a)-(b) shows that the accurate convergence as a function of the iteration number using Algorithm 4.1 decreases when the iteration number increases.

In Fig. 3(a)-(b), we have plotted the exact and computed displacements as a function of $y \in [0, 0.5]$ using Algorithm 4.1. The discrepancy is about 5×10^{-5} near to the corner.

We can observe in Fig. 4(a)-(b) where the exact and computed tractions are plotted as a function of $y \in [0, 0.5]$ using Algorithm 4.1. The discrepancy is about 2.5×10^{-2} near to the corner.

5.2. Example 2. This example deals with the same exact solution as in Eq. (38). This example consists in splitting the domain Ω into two overlap rectangular subdomains $\Omega_1 = (0,1) \times (0,0.5)$ and $\Omega_2 = (0,0.5) \times (0,1)$ with overlap is $(0., 0.5) \times (0, 0.5)$.

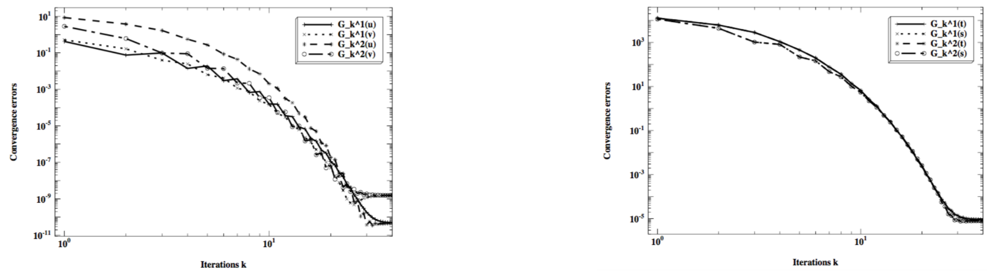

(a) (b)

FIGURE 2. The accuracy errors given by (37) as a function of the number of iterations k on interface γ for Example 1.

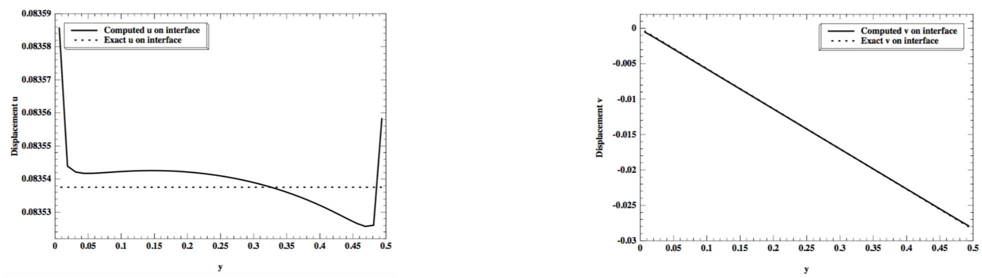

(a) (b)

FIGURE 3. Computed and analytical u, v on interface γ for Example 1.

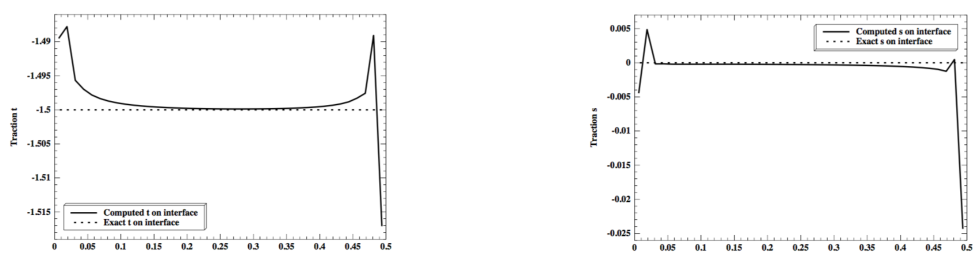

(a) (b)

FIGURE 4. Computed, analytical t, s on interface γ for Example 1.

In Fig. 5, we observe the convergence of calculated solution to exact solution as a function of the iteration number by the use of Algorithm 4.2.

The conclusions drawn from Fig. 5 are graphically enhanced in Figs. 6-10 which show the numerical results obtained using Algorithm 4.2 in comparison with the analytical solutions.

Comparing Algorithm 4.1 and Algorithm 4.2 to solve linear elasticity problem in L-shaped domain, we can see from Figs. 2 and 6 that Algorithm 4.2 requires much less iterations than Algorithm 4.1. The computed solutions are accurate and consistent with respect to increasing the iteration number k.

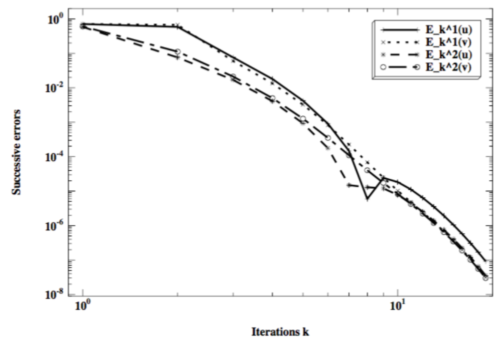

FIGURE 5. the behavior errors given by (33) and (34) as a function of the number of iterations k on part of boundaries γ_2 for Example 2.

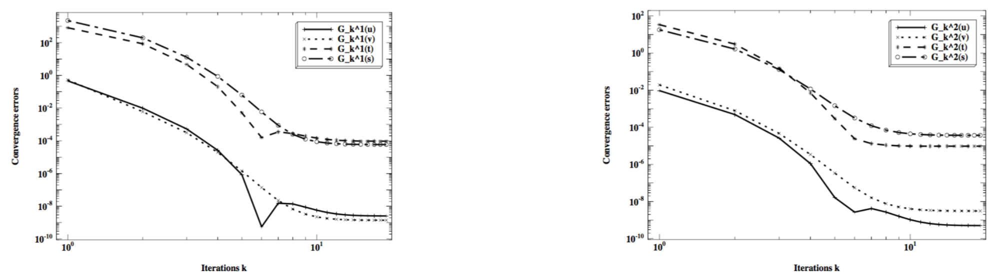

(a) (b)

FIGURE 6. The accuracy errors given by (37) as a function of the number of iterations k on part of boundaries γ_2 for Example 2.

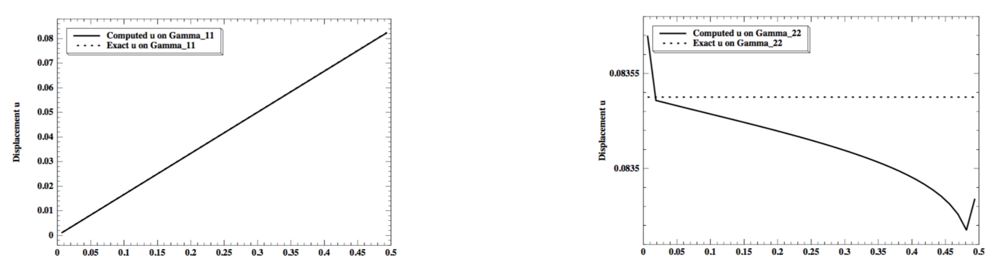

FIGURE 7. Computed, analytical u on γ_1, γ_2 for Example 2.

5.3. Example 3. In this example, we consider the union of two circle geometry domain Ω. This example consists in spliting the domain Ω into two overlap circular subdomains $\Omega_1 = \{(x,y) \in \mathbb{R}^2/(x-0.5)^2 + y^2 = 0.25\}$ and $\Omega_2 = \{(x,y) \in \mathbb{R}^2/(x-0.5(1+\sqrt{2}))^2 + y^2 = 0.25\}$ with overlap is $\Omega_1 \cap \Omega_2$. In order to illustrate the performance of the numerical method described above, we solve the linear elasticity problem (1), in two-circular domain Ω. The exact solution of the direct problem is given by.

$$u(x,y) = \frac{1-2\nu}{2G}\sigma_0 x,\ v(x,y) = \frac{1-2\nu}{2G}\sigma_0 y,\ t(x,y) = \sigma_0 n_1,\ s(x,y) = \sigma_0 n_2 \tag{39}$$

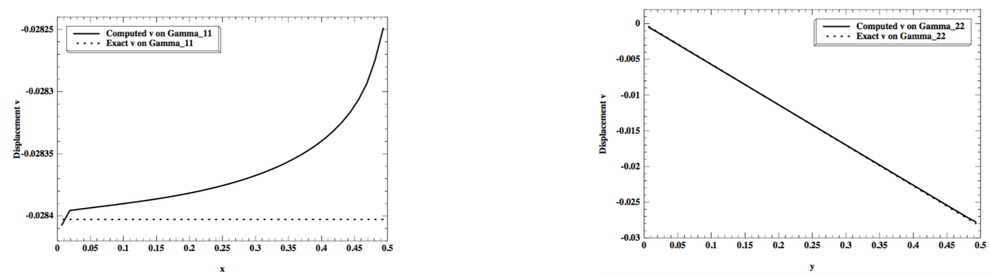

FIGURE 8. Computed and analytical v on γ_1, γ_2 for Example 2.

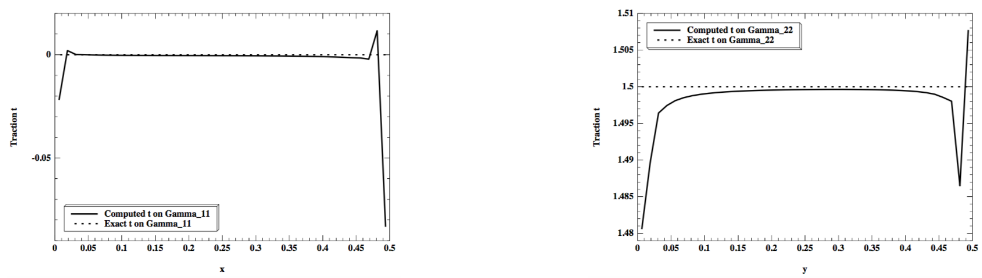

(a) (b)

FIGURE 9. Computed and analytical t on γ_1, γ_2 for Example 2.

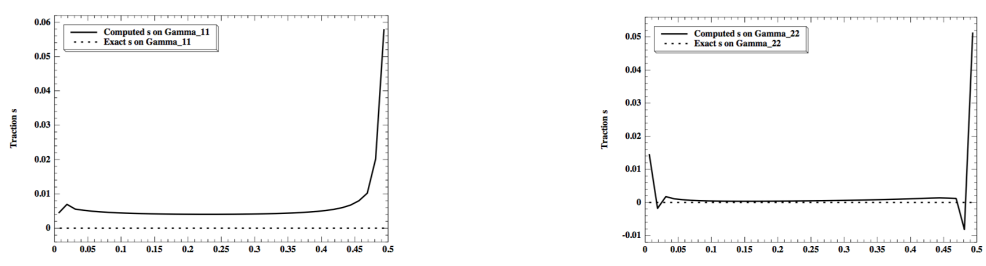

(a) (b)

FIGURE 10. Computed and analytical s on γ_1, γ_2 for Example 2.

with $\sigma_0 = 1.5 \times 10^{10}$, $G = 3.35 \times 10^{10}$ and $\nu = 0.25$.

As a function of the iteration k, four behavior errors are illustrated in Fig. 11 using Algorithm 4.2.

In Fig. 12(a)-(b), we observe the convergence of calculated solution to exact solution as a function of the iteration number by the use of Algorithm 4.2.

The conclusions drawn from Fig. 11 are graphically enhanced in Figs. 13-16 which show the numerical results obtained using Algorithm 4.2 in comparison with the analytical solutions.

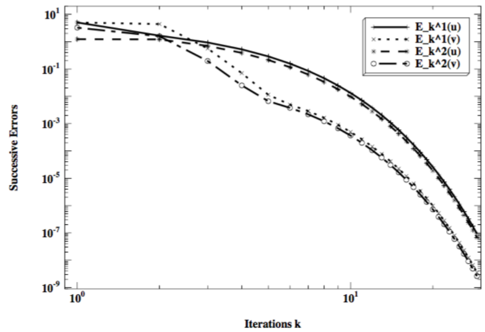

FIGURE 11. The behavior errors given by(33), (34) as a function of the number of iterations k on part of boundaries of Ω_1 and Ω_2 respectively, for Example 3.

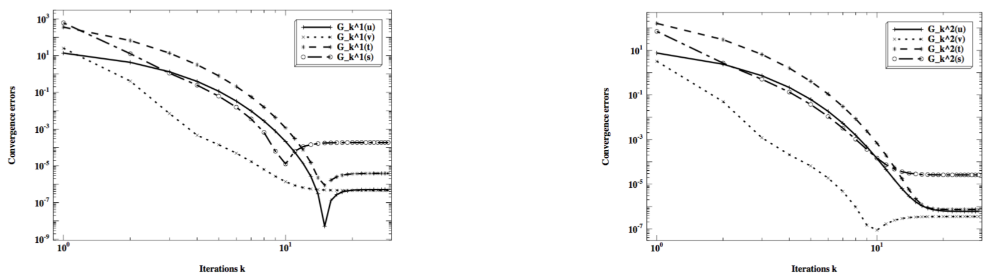

(a) (b)

FIGURE 12. The accuracy errors given by (37) as a function of the number of iterations k on part of boundaries of Ω_1 and Ω_2 respectively, for Example 3.

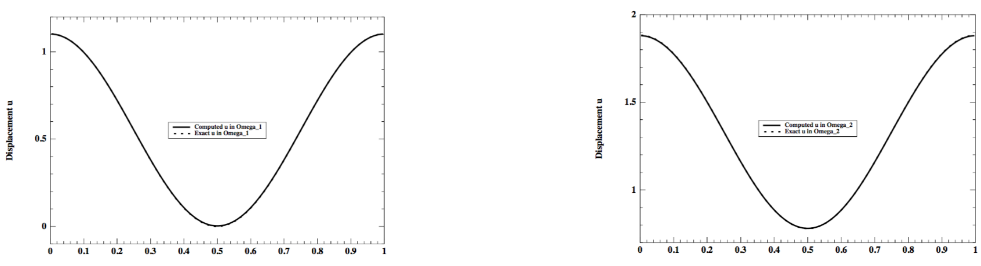

(a) (b)

FIGURE 13. Computed and analytical u in Ω_1, Ω_2 for Example 3.

6. Conclusion

A domain decomposition coupled with Boundary element method was presented to solve linear elasticity equations in complicated geometries. Three examples of domain are given. Stopping and two accuracy criteria given by Eq. (35) for Dirichlet-Neumann method, Eq. (34) for Schwarz method and accuracy criteria given by Eqs.(37) have

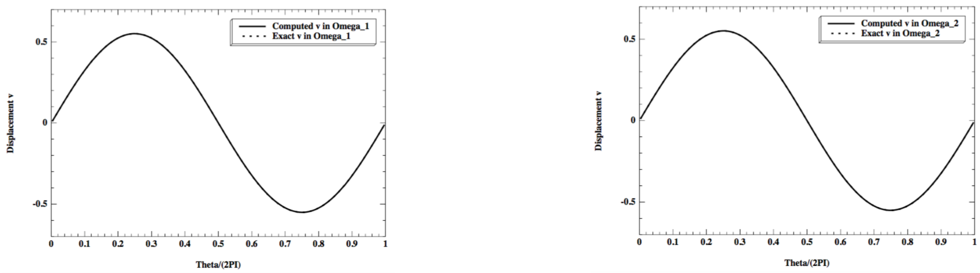

(a) (b)

FIGURE 14. Computed and analytical v in Ω_1, Ω_2 for Example 3.

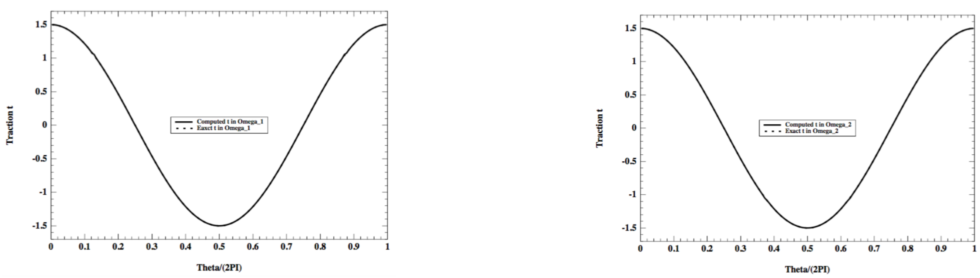

(a) (b)

FIGURE 15. Computed and analytical t in Ω_1, Ω_2 for Example 3.

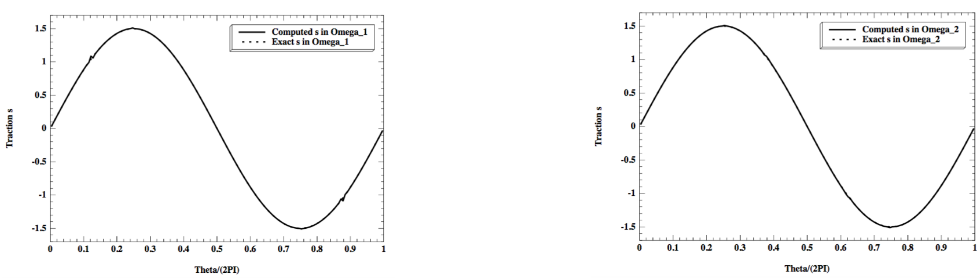

(a) (b)

FIGURE 16. Computed and analytical s in Ω_1, Ω_2 for Example 3.

been used. The numerical results presented in the last section showed that the alternating Algorithm 4.1 and Algorithm 4.2 produces an accurate numerical solution of problems given by Example 1-3 with respect to increasing the number of iterations. Numerical results for Example 1 show that Algorithm 4.2 is more robust than Algorithm 4.1.

References

[1] A. Avudainayagam and C. Vani, A domain decomposition method for biharmonic equation, *Computers and Mathematics with Applications* **40** (2000), 865–876.

[2] M. Barboteu, P. Alart, and M. Vidrascu, A domain decomposition strategy for non-classical frictionless multi-contact problems, Comput. Meth. Appl. Mech. Eng. **190** (2001), 4785–4803.

[3] C. A. Brebbia and J. Dominguez, *Boundary Elements An Introductory course*, Comp. Mech. Pub. McGraw-Hill Book Company, 1992.

[4] T. Bui and V. Popov, Domain decomposition boundary element method with overlapping subdomains, *Eng. Anal. Bound. Elem.* **33** (2009), no. 4, 456–466.

[5] J. Danbk, I. Hlavadek, and J. Nedoma, Domain decomposition for generalized unilateral semicoercive contact problem with given friction in elasticity, *Math. Comput. Simulation* **68** (2005), no. 3, 271–300.

[6] Y. H. De Roeck, P. Le Tallec, and M. Vidrascu, A domain-decomposed solver for nonlinear elasticity, *J. Comput. Methods Appl. Mech. Eng.* **99** (1992), no. 2/3, 187–207.

[7] W.M. Elleithy and H.J. Al-Gahtani, An overlapping domain decomposition approach for coupling the finite and boundary element methods, *Eng. Anal. Bound. Elem.* **24** (2000), no. 5, 391–398.

[8] V. Girault, G.V. Pencheva, M.F. Wheeler, and T.M. Wildey, Domain decomposition for linear elasticity with DG jumps and mortars *Comput. Methods Appl. Mech. Engrg.* **198** (2009), no. 21-26, 1751–1765.

[9] P. Goldfeld, L.F. Pavarino, and O.B. Widlund, Balancing Neumann-Neumann methods for mixed approximations of linear elasticity, *Lect. Notes Comput. Sci. Eng.* **23** (2002), 53–76.

[10] A. Janka, Algebraic domain decomposition solver for linear elasticity Proceedings of the 9th Seminar, Programs and Algorithms of Numerical Mathematics, *Appl. Math.* **44** (1999), no. 6, 435–458.

[11] Y. Jun and T. Mai, Numerical analysis of the rectangular domain decomposition method, *Comm. Numer. Methods Engrg.* **25** (2009), no. 7, 810–826.

[12] A. Klawonn and O. B. Widlund, A domain decomposition method with Lagrange multipliers and inexact solvers for linear elasticity, *SIAM J. Sci. Comput.* **22** (2000), no.4, 1199–1219.

[13] P. Luo and G. Liang, Domain decomposition methods with nonmatching grids for the unilateral problem, *J. Comput. Math.* **20** (2002), 193–202.

[14] A. Nachaoui, J. Abouchabaka, and N. Rafalia, Parallel solvers for the depletion region identification in metal semiconductor field effect transistors, *Numer. Algorithms* **40** (2005), no. 2, 187–199.

[15] L.F. Pavarino, and A. Toselli, *Recent Developments in Domain Decomposition Methods*, Lecturer Notes in Computer Sci. Eng. **23**, Springer Verlag, 2002.

[16] T. Panzeca, M. Salerno, and S. Terravecchia, Domain decomposition in the symmetric boundary element analysis, *Comput. Mech.* **28** (2002), no. 3-4, 191–201.

[17] A. Quarteroni and A. Valli, *Domain decomposition methods for partial differential equations*, Oxford University Press, Oxford, 1999.

[18] P. Le Tallec, Domain decomposition methods in computational mechanics, *Comput. Mech. Adv.* **1** (1994), 121–220.

[19] A. Toselli and O. Widlund, *Domain decomposition methods - algorithms and theory*, Springer Series in Computational Mathematics 34, Berlin Springer, 2005.

[20] P.N. Vabishchevich, Domain decomposition methods with overlapping subdomains for the time-dependent problems of mathematical physics, *Comput. Methods Appl. Math.* **8** (2008), no. 4, 393–405.

(Abdellatif Ellabib) Laboratoire de Mathématiques Appliquées et Informatique, Faculté des Sciences et Techniques de Marrakech, Université Cadi Ayyad, B.P 549, Marrakech, Morocco.
E-mail address: a.ellabib@uca.ma

(Abdeljalil Nachaoui) Laboratoire de Mathématiques Jean Leray, UMR 6629, Université de Nantes/CNRS/ECN, 2 rue de la Houssinière, BP 92208, 44322 Nantes, France.
E-mail address: nachaoui@univ-nantes.fr